

Global extraction of unpolarized quark TMDs at N³LL

The MAP Collaboration

Presented at DIS2022: XXIX International Workshop on Deep-Inelastic Scattering and Related Subjects, Santiago de Compostela, Spain, May 2-6 2022.

Matteo Cerutti,^{1,2,*} Alessandro Bacchetta,^{1,2} Valerio Bertone,³ Chiara Bissolotti,^{1,4} Giuseppe Bozzi,^{5,6} Marco Radici,² and Andrea Signori^{7,8}

¹*Dipartimento di Fisica, Università di Pavia, via Bassi 6, I-27100 Pavia, Italy*

²*INFN - Sezione di Pavia, via Bassi 6, I-27100 Pavia, Italy*

³*IRFU, CEA, Université Paris-Saclay, F-91191 Gif-sur-Yvette, France*

⁴*HEP Division, Argonne National Laboratory,*

9700 S. Cass Avenue, Lemont, IL-60439 USA

⁵*Dipartimento di Fisica, Università di Cagliari,*

Cittadella Universitaria, I-09042 Monserrato (CA), Italy

⁶*INFN - Sezione di Cagliari, Cittadella Universitaria, I-09042 Monserrato (CA), Italy*

⁷*Dipartimento di Fisica, Università di Torino, via P. Giuria 1, I-10125 Torino, Italy*

⁸*INFN - Sezione di Torino, via P. Giuria 1, I-10125 Torino, Italy*

We present the most recent extraction of unpolarized transverse-momentum-dependent (TMD) parton distribution functions (PDFs) and TMD fragmentation functions (FFs) from global data sets of Semi-Inclusive Deep-Inelastic Scattering (SIDIS) and Drell-Yan. The fit is performed at the (next-to-)³leading logarithmic accuracy in the resummation of q_T -logarithms and features flexible non-perturbative functions, which allow to reach a very good agreement with the experimental data. In particular, we address the tension between the low-energy SIDIS data and the theory predictions, and explore the impact of the precise LHC data on the fit results.

I. INTRODUCTION

A crucial step towards understanding the interactions among quarks and gluons and the phenomenon of confinement can be achieved by charting multi-dimensional maps of the internal structure of nucleons.

Transverse-momentum-dependent distributions (TMDs) encode information about the three-dimensional distribution of quarks in momentum space. The level of sophistication of a TMD extraction from experimental data can be described by the following features: the number of included data from different experiments, and the perturbative accuracy in the resummation of large q_T -logarithms reached in the theoretical formalism. In this analysis, we include 2031 experimental data and we push the accuracy of the calculation to what we will refer to as N³LL[−].¹

This contribution is a summary of the results extensively discussed in Ref. [1]. At present, the extractions of Ref. [1–3] are the only global analyses available on the market, namely they combine SIDIS and DY data in a full-fledged TMD fit. These fits rely on the universality of the partonic distributions and take advantage of using different processes to constrain them better.

As discussed in the next section, describing SIDIS data at moderate to low scales up to N²LL and N³LL[−] is very challenging. We solve this issue by fixing the normalization of the TMD predictions through a multiplicative prefactor which compares their integral upon transverse momentum to the corresponding cross section calculated in collinear factorization. With this prefactor, we fix the normalization in a theoretically well-justified way, which is also independent of the results of the fit.

The reduced- χ^2 of our baseline fit, performed at N³LL[−] using 2031 data points, is $\chi^2/N_{\text{dat}} = 1.06$.

II. FORMALISM

A. SIDIS cross section

In the limit where leptonic and hadronic masses can be neglected, the differential cross section for unpolarized SIDIS at small transverse momentum [2, 4] reads:

$$\frac{d\sigma^{\text{SIDIS}}}{dx dz d|\mathbf{q}_T| dQ} = \frac{8\pi^2 \alpha^2 z^2 |\mathbf{q}_T|}{x Q^3} \left[1 + \left(1 - \frac{Q^2}{xs} \right)^2 \right] F_{UU,T}(x, z, \mathbf{q}_T^2, Q), \quad (1)$$

*Electronic address: matteo.cerutti@pv.infn.it – ORCID: 0000-0001-7238-5657

¹ Including NNLO FFs one would reach the full N³LL accuracy.

where x, z are the light-cone fractions related to the collinear momenta of the incoming and outgoing quarks, respectively [4]; q is the 4-momentum of the exchanged virtual photon, whose transverse component in the frame where the incoming and outgoing hadrons are collinear is denoted as \mathbf{q}_T , and for which $Q^2 = -q^2 > 0$; α is the QED coupling constant. Since we focus only on the small transverse momentum region $|\mathbf{q}_T| \ll Q$ (i.e. the TMD region), in Eq. (1) we neglect the contributions from fixed-order calculations at high $|\mathbf{q}_T|$ and the matching of these to the TMD region.

The unpolarized SIDIS structure function $F_{UU,T}$ is defined as [4]:

$$F_{UU,T}(x, z, |\mathbf{q}_T|, Q) = \frac{x}{2\pi} \mathcal{H}(Q, \mu) \sum_a e_a^2 \int_0^{+\infty} d|\mathbf{b}_T| |\mathbf{b}_T| J_0(|\mathbf{b}_T| |\mathbf{q}_T|) \hat{f}_1^a(x, \mathbf{b}_T^2; Q, Q^2) \hat{D}_1^{a \rightarrow h}(z, \mathbf{b}_T^2; Q, Q^2) \quad (2)$$

where the sum runs over quarks and antiquarks a . \mathcal{H} is the SIDIS hard function and μ is the renormalization scale. The $\hat{f}_1^a(x, \mathbf{b}_T^2; Q, Q^2)$ and $\hat{D}_1^{a \rightarrow h}(z, \mathbf{b}_T^2; Q, Q^2)$ are, respectively, the Fourier transforms of the unpolarized TMD PDF for a quark a in a proton, $f_1^a(x, \mathbf{k}_\perp^2; Q, Q^2)$, and of the TMD FF for a quark with flavor a fragmenting into a hadron with flavor h , $D_1^{a \rightarrow h}(z, \mathbf{z}_\perp^2; Q, Q^2)$. The variable \mathbf{b}_T is conjugated via Fourier transform to the transverse momentum \mathbf{q}_T (and to the partonic transverse momenta \mathbf{k}_\perp and \mathbf{p}_\perp , such that $\mathbf{q}_T = \mathbf{p}_\perp - \mathbf{k}_\perp$). The Q and Q^2 -dependence of both the TMD PDF and FF is introduced by the ultraviolet and rapidity renormalization of the TMDs (see Sec. II C for more details on the scale choices).

The observable provided by the HERMES and COMPASS collaborations is the multiplicity, namely the ratio of the SIDIS cross section over the DIS one

$$M(x, z, |\mathbf{P}_{hT}|, Q) = \frac{d\sigma^{\text{SIDIS}}}{dx dz d|\mathbf{P}_{hT}| dQ} \bigg/ \frac{d\sigma^{\text{DIS}}}{dx dQ} \quad (3)$$

where \mathbf{P}_{hT} is the transverse momentum of the observed hadron in the Breit frame, which is related to \mathbf{q}_T as [5]:

$$\mathbf{q}_T = -\mathbf{P}_{hT}/z. \quad (4)$$

In Ref. [2] it was demonstrated that TMD factorization at NLL accuracy is able to successfully reproduce the normalization and shape of HERMES multiplicities and the shape of the available COMPASS multiplicities. At variance with Ref. [3], we find a significant tension between the experimental values for the SIDIS multiplicities and the calculations in TMD factorization beyond NLL. This tension has been observed independently by other groups and documented, for example, in Ref. [6]. We propose to modify the normalization of the N²LL and N³LL predictions to recover a good agreement with data. An extended discussion of this issue can be found in Ref. [7]. The proposed solution consists in introducing the following normalization factor:

$$\omega(x, z, Q) = \frac{d\sigma}{dx dz dQ} \bigg/ \int d^2 \mathbf{q}_T W, \quad (5)$$

where the numerator is the cross section for SIDIS in collinear factorization and the W term in the denominator coincides with Eq. (1) (see also the terminology of Ref. [5]). This prefactor accounts for the difference between the integral of the \mathbf{q}_T -dependent SIDIS cross section at low transverse momentum and the collinear cross section at a given order in perturbation theory. Within the scope of our analysis, which is limited to the small transverse momentum region, the \mathbf{q}_T -differential cross section is approximated with the TMD calculation. This prefactor does not depend on \mathbf{q}_T or any of the fit parameters (for more details, see Ref. [1]) and is different from 1 beyond NLL. As a consequence, the theoretical expression for the multiplicity becomes:

$$\frac{d\sigma_{\omega}^{\text{SIDIS}}}{dx dz d|\mathbf{q}_T| dQ} = \omega(x, z, Q) \frac{d\sigma^{\text{SIDIS}}}{dx dz d|\mathbf{q}_T| dQ}. \quad (6)$$

B. Drell-Yan cross sections

The cross section for Drell-Yan reads:

$$\frac{d\sigma^{\text{DY/Z}}}{d|\mathbf{q}_T| dy dQ} = \frac{16\pi^2 \alpha^2}{9Q^3} |\mathbf{q}_T| \mathcal{P} F_{UU}^1(x_A, x_B, |\mathbf{q}_T|, Q), \quad (7)$$

where \mathbf{q}_T is the transverse momentum of the intermediate boson, y is its rapidity, and \mathcal{P} is the phase space factor to account for potential cuts on the lepton kinematics [8]. At low transverse momentum $\mathbf{q}_T^2 \ll Q^2 = q^2 > 0$ the structure function can be expressed as a convolution over the partonic transverse momenta of two TMD PDFs:

$$F_{UU}^1(x_A, x_B, |\mathbf{q}_T|, Q) = \frac{x_A x_B}{2\pi} \mathcal{H}(Q, \mu) \sum_a c_a(Q) \int_0^{+\infty} d|\mathbf{b}_T| |\mathbf{b}_T| J_0(|\mathbf{b}_T| |\mathbf{q}_T|) \hat{f}_1^a(x_A, \mathbf{b}_T^2; Q, Q^2) \hat{f}_1^{\bar{a}}(x_B, \mathbf{b}_T^2; Q, Q^2), \quad (8)$$

where $c_a(Q)$ are the electro-weak charges [8], \mathcal{H} is the hard function of the process, μ is the renormalization scale, $x_{A,B}$ are the partonic longitudinal momentum fractions, which, in the small transverse momentum limit, take the values:

$$x_A = \frac{Q}{\sqrt{s}} e^y, \quad x_B = \frac{Q}{\sqrt{s}} e^{-y}. \quad (9)$$

C. Transverse momentum distributions

The evolved TMDs from the initial values of the renormalization and rapidity scales μ_i, ζ_i , to the final values μ_f, ζ_f , read

$$\hat{f}_1^a(x, \mathbf{b}_T^2; \mu_f, \zeta_f) = \hat{f}_1^a(x, \mathbf{b}_T^2; \mu_i, \zeta_i) \exp \left\{ \int_{\mu_i}^{\mu_f} \frac{d\mu}{\mu} \gamma_F \left[\alpha_s(\mu); \frac{\zeta}{\mu^2} \right] \right\} \left(\frac{\zeta_f}{\zeta_i} \right)^{K(|\mathbf{b}_T|, \mu_i)/2}, \quad (10)$$

where α_s is the strong coupling constant and K is the Collins-Soper kernel [5]. The same structure holds for the TMD FF. The scale μ_i can be conveniently fixed as $\mu_b = 2e^{-\gamma_E}/|\mathbf{b}_T|$, and thus Eq. (10) is perturbatively meaningful only at low values of $|\mathbf{b}_T|$. The arbitrary matching to the non-perturbative regime at large $|\mathbf{b}_T|$ is accomplished by modifying the scale μ_b as $\mu_{b*} = 2e^{-\gamma_E}/b_*$, with

$$b_*(|\mathbf{b}_T|, b_{\min}, b_{\max}) = b_{\max} \left(\frac{1 - e^{-|\mathbf{b}_T|^4/b_{\max}^4}}{1 - e^{-|\mathbf{b}_T|^4/b_{\min}^4}} \right)^{1/4}, \quad (11)$$

where

$$b_{\max} = 2e^{-\gamma_E} \text{ GeV}^{-1} \approx 1.123 \text{ GeV}^{-1}, \quad b_{\min} = 2e^{-\gamma_E}/Q. \quad (12)$$

In this way, b_* saturates to b_{\max} at large $|\mathbf{b}_T|$, as suggested by the CSS formalism [5]. At small $|\mathbf{b}_T|$, the arbitrary matching to fixed-order collinear calculations is realized by saturating b_* to b_{\min} . Accordingly, in the limit $|\mathbf{b}_T| \rightarrow 0$ the Sudakov exponent vanishes. For the processes considered in this analysis, it is customary to choose the final scales as $\mu_f^2 = \zeta_f = Q^2$ [5], which explains the Q dependence of the structure functions and of the TMDs in Eqs. (2) and (8). In order to avoid the Landau pole at large $|\mathbf{b}_T|$, the Collins-Soper kernel K needs to be modified by including a correction term, $g_K(\mathbf{b}_T^2)$, for which we choose a specific functional form:

$$K(|\mathbf{b}_T|, \mu_{b*}) = K(b_*, \mu_{b*}) + g_K(|\mathbf{b}_T|), \quad g_K(\mathbf{b}_T^2) = -g_2^2 \frac{\mathbf{b}_T^2}{4}. \quad (13)$$

In order not to affect the perturbative calculation at small $|\mathbf{b}_T|$, the $g_K(\mathbf{b}_T^2)$ needs to vanish in the limit $|\mathbf{b}_T| \rightarrow 0$. The TMD PDF (FF) at the input scales can be factorized on the basis of collinear PDFs (FFs):

$$\hat{f}_1^a(x, b_*, \mu_{b*}, \mu_{b*}^2) = \sum_b \int_x^1 \frac{dx'}{x'} C^{ab}(x', b_*, \mu_{b*}, \mu_{b*}^2) f_1^b\left(\frac{x}{x'}, \mu_{b*}\right) \equiv [C \otimes f_1](x, b_*, \mu_{b*}, \mu_{b*}^2), \quad (14)$$

where the sum runs over quarks, antiquarks, and the gluon. The matching coefficients C are determined as a perturbative expansion in powers of $\alpha_s(\mu_{b*})$. At large $|\mathbf{b}_T|$ we introduce a flavor-independent non-perturbative factor multiplying the matching in Eq. (14). For the TMD PDF it is defined as:

$$f_{1NP}(x, \mathbf{b}_T^2; \zeta, Q_0) = \frac{g_1(x) e^{-g_1(x) \frac{\mathbf{b}_T^2}{4}} + \lambda^2 g_{1B}^2(x) \left[1 - g_{1B}(x) \frac{\mathbf{b}_T^2}{4} \right] e^{-g_{1B}(x) \frac{\mathbf{b}_T^2}{4}} + \lambda_2^2 g_{1C}(x) e^{-g_{1C}(x) \frac{\mathbf{b}_T^2}{4}}}{g_1(x) + \lambda^2 g_{1B}^2(x) + \lambda_2^2 g_{1C}(x)} \left[\frac{\zeta}{Q_0^2} \right]^{g_K(\mathbf{b}_T^2)/2}, \quad (15)$$

and for the TMD FF, instead, the form is:

$$D_{1NP}(z, \mathbf{b}_T^2; \zeta, Q_0) = \frac{g_3(z) e^{-g_3(z) \frac{\mathbf{b}_T^2}{4z^2}} + \frac{\lambda_F}{z^2} g_{3B}^2(z) \left[1 - g_{3B}(z) \frac{\mathbf{b}_T^2}{4z^2} \right] e^{-g_{3B}(z) \frac{\mathbf{b}_T^2}{4z^2}}}{g_3(z) + \frac{\lambda_F}{z^2} g_{3B}^2(z)} \left[\frac{\zeta}{Q_0^2} \right]^{g_K(\mathbf{b}_T^2)/2}. \quad (16)$$

The non-perturbative factors f_{1NP} , $D_{1NP} \rightarrow 1$ for $\mathbf{b}_T \rightarrow 0$. The g_i functions account for the kinematic dependence of the widths of the distributions:

$$g_{\{1,1B,1C\}}(x) = N_{\{1,1B,1C\}} \frac{x^{\sigma_{\{1,2,3\}}}(1-x)^{\alpha_{\{1,2,3\}}^2}}{\hat{x}^{\sigma_{\{1,2,3\}}}(1-\hat{x})^{\alpha_{\{1,2,3\}}^2}}, \quad g_{\{3,3B\}}(z) = N_{\{3,3B\}} \frac{(z^{\beta_{\{1,2\}}} + \delta_{\{1,2\}}^2)(1-z)^{\gamma_{\{1,2\}}^2}}{(\hat{z}^{\beta_{\{1,2\}}} + \delta_{\{1,2\}}^2)(1-\hat{z})^{\gamma_{\{1,2\}}^2}}, \quad (17)$$

where $\hat{x} = 0.1$, $\hat{z} = 0.5$, and $Q_0 = 1 \text{ GeV}^2$.

In total there are 21 free parameters: 1 associated to the non-perturbative part of TMD evolution (Eq. (13)), 11 related to the non-perturbative part of the TMD PDF (Eqs. (15), (17)), 9 for the non-perturbative part of the TMD FF (Eqs. (16), (17)).

III. EXPERIMENTAL DATA

This fit is based on the analysis of the “global” set of experimental data available to extract unpolarized TMDs, namely SIDIS, Drell-Yan (and Z -boson production). As already mentioned, experimental data for electron-positron annihilation into two hadrons are not available yet. Moreover, we do not include in this analysis data from processes involving jet-based quantities, since they significantly differ from the involved formalism, and data for W -boson production, whose interpretation in TMD factorization presents specific challenges (e.g. the definition of the hard scale) and opportunities (e.g. the access to the flavor structure of the TMDs [9]). The number of data points included in this analysis is 2031, of which 1547 come from SIDIS measured by the HERMES and COMPASS collaborations. The first provides unpolarized multiplicities for scattering off a proton and deuteron target, with detected final-state positive and negative pions and kaons. The second provides multiplicities for scattering off a deuteron with detected final-state charged hadrons. The rest of the data is for Drell-Yan, both in the collider mode (from the ATLAS, CMS, CDF, D0, STAR, PHENIX collaborations) and in the fixed-target mode at low energy (from the E288, E605, E772 collaborations).

IV. RESULTS

The present analysis is performed at an approximate N^3 LL perturbative accuracy [1]. We rely on the following choices for the collinear PDFs and FFs: MMHT2014nnlo68cl for the proton PDFs (the deuteron is described with the same set and isospin symmetry), DSS14-NLO for the quark-to-pion FFs, DSS17-NLO for the quark-to-kaon FFs. On top of the experimental uncertainties, we associate a theoretical error to the observable related to the nature of the collinear set used in this analysis. We compute this error using the Hessian method. Since we observe that PDF and FF uncertainties are significantly correlated across bins, we decompose them into a correlated part (80% of the total) and an uncorrelated part (the remaining 60%) to be combined in quadrature.

In order to restrict the analysis to the small transverse momentum region, we impose the following cuts:

$$|\mathbf{q}_T|_{\text{DY/Z}} < 0.20 Q, \quad |\mathbf{P}_{hT}|_{\text{SIDIS}} < \min[\min[c_1 Q, c_2 zQ] + c_3 \text{ GeV}, zQ], \quad (18)$$

where $c_1 = 0.2$, $c_2 = 0.5$, $c_3 = 0.3$. In the SIDIS case, the structure of Eq. (18) guarantees that $|\mathbf{q}_T| < Q$.

By fitting 21 free parameters to the 2031 experimental data, we obtain a χ^2/N_{dat} of 1.06. We perform the error analysis with the replica method, namely by fitting an ensemble of 250 Monte Carlo replicas of the dataset.² We refer the reader to Ref. [1] for more details about the fitting procedure and the comparison between experimental data and the theory predictions.

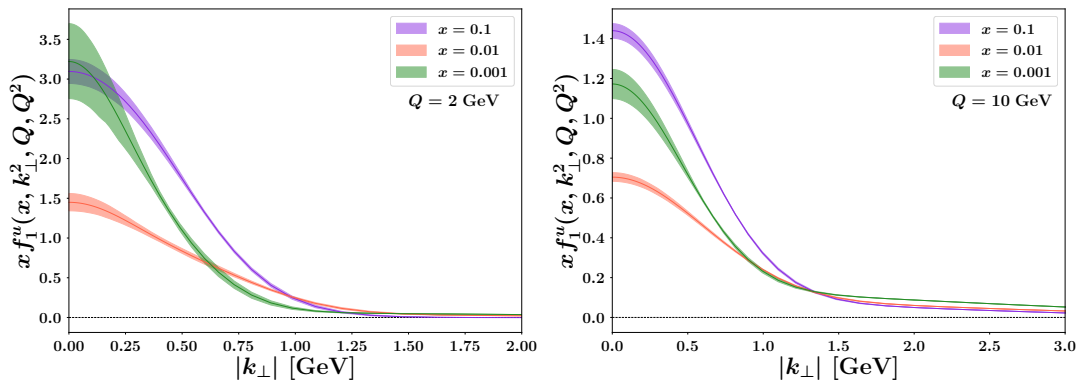


FIG. 1: The TMD PDF of the up quark in a proton at $\mu = \sqrt{\zeta} = Q = 2$ GeV (left panel) and 10 GeV (right panel) as a function of the partonic transverse momentum $|\mathbf{k}_\perp|$ for $x = 0.001, 0.01$ and 0.1 . The uncertainty bands represent the 68% confidence level (CL).

In Fig. 1, we show an example of the extracted unpolarized TMD PDFs for an up quark in a proton, including both perturbative and non-perturbative components (see Ref. [1] for the visualization of TMD FFs). The shape of the non-perturbative parts is crucial for a correct description of the data. In Fig. 1, one can appreciate the significant role played by the weighted Gaussian and by the second Gaussian in Eq. (15), which may reflect the underlying contribution from different (spin) configurations.

² The aforementioned value of the χ^2/N_{dat} is related to the original (unfluctuated) dataset.

It is interesting to see the result for the Collins–Soper kernel [5] that drives the evolution of TMDs in terms of the rapidity scale ζ .

In Fig. 2, we show the Collins–Soper kernel as a function of $|\mathbf{b}_T|$ at the scale $\mu = 2$ GeV for the MAPTMD22 analysis and for four other analyses [2, 3, 8, 10]. The solid lines at low $|\mathbf{b}_T|$ correspond to the perturbative contribution, which differs due to the different logarithmic accuracies of the various analyses.

The b_* prescription modifies the curves starting from $|\mathbf{b}_T| \approx 1$ GeV $^{-1}$. The behavior at high $|\mathbf{b}_T|$ is driven by the choice of the parameterization of g_K and, so, is different for the various analyses.

The b_* variable saturates to $b_{\min} \approx 1.123/Q$ in this analysis and also in Ref. [2]. This implies that at low $|\mathbf{b}_T|$ the Collins–Soper kernel saturates to a finite value, as indicated by the corresponding dashed lines.

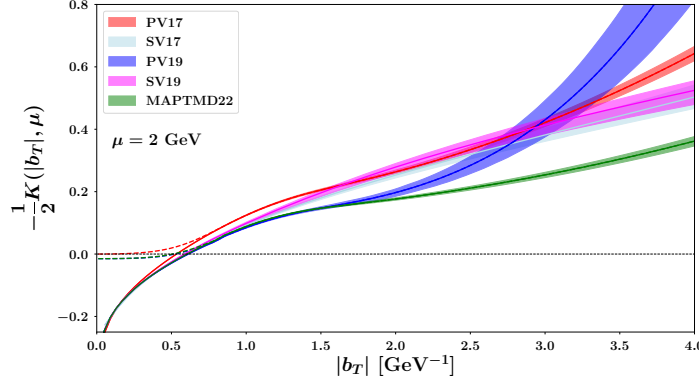


FIG. 2: The Collins–Soper kernel as a function of $|\mathbf{b}_T|$ at a scale $\mu = 2$ GeV from the present analysis (MAPTMD22), compared with the PV17 [2], SV17 [10], PV19 [8], and SV19 [3] analyses. For the MAPTMD22, PV17, and PV19 curves, the uncertainty bands represent the 68% CL. Dashed lines show the effect of including the b_{\min} -prescription.

The complete list of results (theory summary, global statistical estimators, etc.) obtained from the fit presented in this contribution will be available at the following public git repository:

<https://github.com/MapCollaboration/NangaParbat>

Acknowledgments. This work is supported by the European Union’s Horizon 2020 programme under grant agreement No. 824093 (STRONG2020). C.B. is supported by the DOE contract DE-AC02-06CH11357. A.S. acknowledges support from the European Commission through the Marie Skłodowska-Curie Action SquHadron (grant agreement ID: 795475).

-
- [1] A. Bacchetta, V. Bertone, C. Bissolotti, G. Bozzi, M. Cerutti, F. Piacenza et al., *Unpolarized Transverse Momentum Distributions from a global fit of Drell-Yan and Semi-Inclusive Deep-Inelastic Scattering data*, 2206.07598.
 - [2] A. Bacchetta, F. Delcarro, C. Pisano, M. Radici and A. Signori, *Extraction of partonic transverse momentum distributions from semi-inclusive deep-inelastic scattering, Drell-Yan and Z-boson production*, *JHEP* **06** (2017) 081, [1703.10157].
 - [3] I. Scimemi and A. Vladimirov, *Non-perturbative structure of semi-inclusive deep-inelastic and Drell-Yan scattering at small transverse momentum*, *JHEP* **06** (2020) 137, [1912.06532].
 - [4] A. Bacchetta, M. Diehl, K. Goeke, A. Metz, P. J. Mulders and M. Schlegel, *Semi-inclusive deep inelastic scattering at small transverse momentum*, *JHEP* **02** (2007) 093, [hep-ph/0611265].
 - [5] J. Collins, *Foundations of perturbative QCD*, vol. 32. Cambridge University Press, 11, 2013.
 - [6] J. Osvaldo Gonzalez-Hernandez, *Comments on the perturbative and non-perturbative contributions in unpolarized SIDIS*, *PoS DIS2019* (2019) 176.
 - [7] F. Piacenza, *Perturbative and nonperturbative QCD regimes in transverse-momentum dependent observables*. PhD thesis, Università Di Pavia, Pavia U., 2020.
 - [8] A. Bacchetta, V. Bertone, C. Bissolotti, G. Bozzi, F. Delcarro, F. Piacenza et al., *Transverse-momentum-dependent parton distributions up to N^3LL from Drell-Yan data*, *JHEP* **07** (2020) 117, [1912.07550].
 - [9] A. Bacchetta, G. Bozzi, M. Radici, M. Ritzmann and A. Signori, *Effect of Flavor-Dependent Partonic Transverse Momentum on the Determination of the W Boson Mass in Hadronic Collisions*, *Phys. Lett. B* **788** (2019) 542–545, [1807.02101].
 - [10] I. Scimemi and A. Vladimirov, *Analysis of vector boson production within TMD factorization*, *Eur. Phys. J. C* **78** (2018) 89, [1706.01473].